

## Supporting Information

# A wide-bandgap copolymer donor with a 5-methyl-4H-dithieno[3,2-e:2',3'-g]isoindole-4,6(5H)-dione unit

Anxin Sun<sup>1, 2, ‡</sup>, Jingui Xu<sup>2, 3, ‡</sup>, Guanhua Zong<sup>2</sup>, Zuo Xiao<sup>2, †</sup>, Yong Hua<sup>1, †</sup>, Bin Zhang<sup>3, †</sup>, and Liming Ding<sup>2, †</sup>

<sup>1</sup>*Yunnan Key Laboratory for Micro/Nano Materials & Technology, School of Materials and Energy, Yunnan University, Kunming 650091, China*

<sup>2</sup>*Center for Excellence in Nanoscience (CAS), Key Laboratory of Nanosystem and Hierarchical Fabrication (CAS), National Center for Nanoscience and Technology, Beijing 100190, China*

<sup>3</sup>*School of Materials Science and Engineering, Changzhou University, Changzhou 213164, China*

Correspondence to: Z Xiao, xiaoz@nanoctr.cn; Y Hua, huayong@ynu.edu.cn; B Zhang, msbinzhang@outlook.com; L M Ding, ding@nanoctr.cn

<sup>‡</sup> Anxin Sun and Jingui Xu contributed equally to this work.

## 1. General characterization

<sup>1</sup>H and <sup>13</sup>C NMR spectra were measured on a Bruker Avance-400 spectrometer. Absorption spectra were recorded on a Shimadzu UV-1800 spectrophotometer. Cyclic voltammetry was done by using a Shanghai Chenhua CHI620D voltammetric analyzer under argon in an anhydrous acetonitrile solution of tetra-n-butylammonium hexafluorophosphate (0.1 M). A glassy-carbon electrode was used as the working electrode, a platinum-wire was used as the counter electrode, and a Ag/Ag<sup>+</sup> electrode was used as the reference electrode. Polymers were coated onto glassy-carbon electrode and all potentials were corrected against Fc/Fc<sup>+</sup>. AFM was performed on a Multimode microscope (Veeco) by using tapping mode.

## 2. DFT

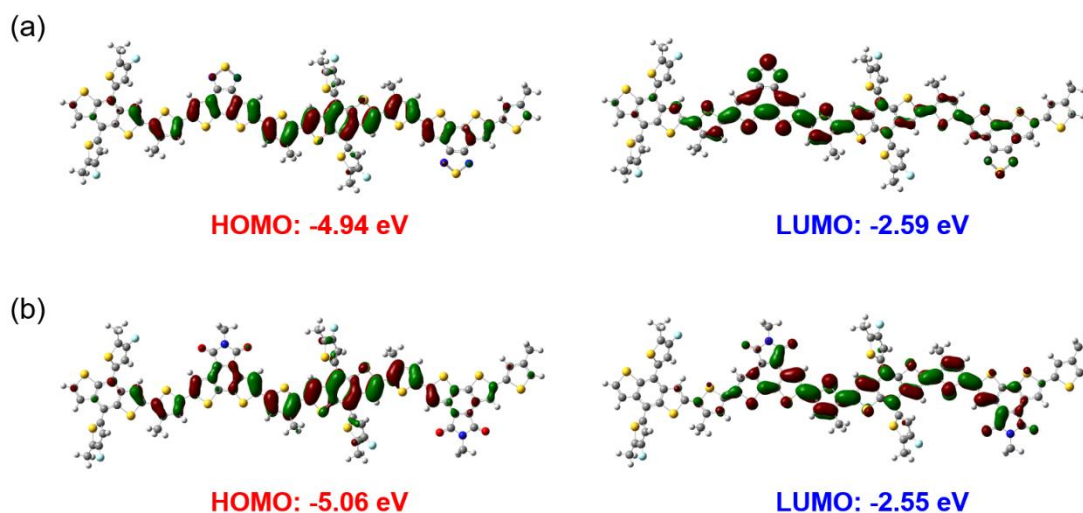


Fig. S1 DFT-predicted HOMO and LUMO for (a) D18 and (b) P1.

## 3. Synthesis

All reagents were purchased from J&K Co., Aladdin Co., Innochem Co., Derthon Co., SunaTech Co. and other commercial suppliers. N3 was purchased from eFlexPV Co. All reactions dealing with air- or moisture-sensitive compounds were carried out by using standard Schlenk techniques.

**Compound 1.** To a solution of 3,4-dibromo-1-methyl-1H-pyrrole-2,5-dione (2.31 g, 8.2 mmol) and tributyl(thiophen-3-yl)stannane (8.99 g, 22.9 mmol) in DMF (45 mL) was added Pd(PPh<sub>3</sub>)<sub>4</sub> (497 mg, 0.41 mmol) under N<sub>2</sub>. The mixture was heated to reflux and stirred overnight. After removal of the solvent, the crude product was purified via column chromatography (silica gel) by using CH<sub>2</sub>Cl<sub>2</sub> as eluent to give **compound 1** as a yellow solid (1.97 g, 83%). <sup>1</sup>H NMR (CDCl<sub>3</sub>, 400 MHz, δ/ppm): 7.98 (dd, *J*<sub>1</sub> = 3.2 Hz, *J*<sub>2</sub> = 1.2 Hz, 2H), 7.34 (dd, *J*<sub>1</sub> = 5.2 Hz, *J*<sub>2</sub> = 2.8 Hz, 2H), 7.25 (dd, *J*<sub>1</sub> = 4.8 Hz, *J*<sub>2</sub> = 1.2 Hz, 2H), 3.12 (s, 3H). <sup>13</sup>C NMR (CDCl<sub>3</sub>, 100 MHz, δ/ppm): 171.02, 129.37, 129.30, 129.27, 127.52, 125.76, 24.17. EI MS (*m/z*): C<sub>13</sub>H<sub>9</sub>NO<sub>2</sub>S<sub>2</sub> (M<sup>+</sup>) calc. 275.34, found 275.

**MDTID.** To a solution of compound 1 (1.00 g, 3.6 mmol) in dry CH<sub>2</sub>Cl<sub>2</sub> (200 mL) was added FeCl<sub>3</sub> (4.71 g, 29.1 mmol) under N<sub>2</sub>. The mixture was stirred at room temperature for 5 h. Then, the resulting mixture was filtered and the filtrate was collected. After removal of the solvent, the residue was washed with n-hexane to give **MDTID** as a yellow solid (424 mg, 43%). <sup>1</sup>H NMR (CDCl<sub>3</sub>, 400 MHz, δ/ppm): 8.11 (d, *J* = 5.6 Hz, 2H), 7.70 (d, *J* = 5.2 Hz, 2H), 3.24 (s, 3H). <sup>13</sup>C NMR (CDCl<sub>3</sub>, 100 MHz, δ/ppm): 169.06, 139.51, 130.75, 128.83, 123.71, 122.35, 23.79. EI MS (*m/z*): C<sub>13</sub>H<sub>7</sub>NO<sub>2</sub>S<sub>2</sub> (M<sup>+</sup>) calc. 273.32, found 273.

**MDTID-Br.** To a solution of MDTID (230 mg, 0.84 mmol) in  $\text{CHCl}_3$  (23 mL) were added NBS (320 mg, 1.80 mmol) and  $\text{H}_2\text{SO}_4$  (0.7 mL). The mixture was stirred at room temperature for 30 min. Another portion of NBS (76 mg, 0.427 mmol) and  $\text{H}_2\text{SO}_4$  (0.2 mL) were added. After 1 h, methanol/water (20/1) was added to quench the reaction. The resulting mixture was filtered to give **MDTID-Br** as a yellow solid (325 mg, 90%). Due to the extremely low solubility of MDTID-Br, NMR data were not acquired. MALDI-TOF MS (m/z):  $\text{C}_{13}\text{H}_5\text{Br}_2\text{NO}_2\text{S}_2$  ( $\text{M}^+$ ) calc. 431.12, found 432.21.

**Compound 2.** To a solution of MDTID-Br (300 mg, 0.70 mmol) and tributyl(4-(2-butyloctyl)thiophen-2-yl)stannane (944 mg, 1.74 mmol) in toluene (10 mL) and DMF (2 mL) was added  $\text{Pd}(\text{PPh}_3)_4$  (82 mg, 0.07 mmol) under  $\text{N}_2$ . The mixture was heated to reflux and stirred overnight. After cooling to room temperature, the mixture was poured into water and extracted with petroleum ether. The combined organic layer was dried over anhydrous  $\text{Na}_2\text{SO}_4$ . After removal of the solvent, the crude product was purified via column chromatography (silica gel) by using  $\text{CH}_2\text{Cl}_2$ :petroleum ether (1:2) as eluent to give **compound 2** as a yellow oil (220 mg, 41%).  $^1\text{H}$  NMR ( $\text{CDCl}_3$ , 400 MHz,  $\delta$ /ppm): 7.83 (s, 2H), 7.12 (s, 2H), 6.92 (s, 2H), 3.10 (s, 3H), 2.55 (d,  $J = 6.8$  Hz, 4H), 1.66-1.64 (m, 2H), 1.34-1.28 (m, 32H), 0.94-0.88 (m, 12H).  $^{13}\text{C}$  NMR ( $\text{CDCl}_3$ , 100 MHz,  $\delta$ /ppm): 168.69, 143.25, 140.95, 137.39, 135.50, 131.76, 127.95, 122.93, 122.54, 116.69, 38.83, 34.93, 33.30, 32.97, 31.92, 29.71, 28.84, 26.59, 23.61, 23.07, 22.70, 14.17, 14.14. MALDI-TOF MS (m/z):  $\text{C}_{45}\text{H}_{59}\text{NO}_2\text{S}_2$  ( $\text{M}^+$ ) calc. 774.21, found 774.84.

**M1.** To a solution of compound 2 (220 mg, 0.28 mmol) in  $\text{CHCl}_3$  (25 mL) was added NBS (106 mg, 0.60 mmol). The mixture was stirred for 2 h. Then methanol was added and the resulting mixture was filtered. The precipitate was collected and was purified via column chromatography (silica gel) by using  $\text{CH}_2\text{Cl}_2$ :petroleum ether (1:2) as eluent to give **M1** as a yellow solid (215 mg, 81%).  $^1\text{H}$  NMR ( $\text{CDCl}_3$ , 400 MHz,  $\delta$ /ppm): 7.96 (s, 2H), 7.06 (s, 2H), 3.23 (s, 3H), 2.53 (d,  $J = 7.2$  Hz, 4H), 1.72-1.69 (m, 2H), 1.35-1.26 (m, 32H), 0.93-0.88 (m, 12H).  $^{13}\text{C}$  NMR ( $\text{CDCl}_3$ , 100 MHz,  $\delta$ /ppm): 168.50, 142.72, 139.91, 137.21, 135.17, 131.69, 127.37, 123.11, 116.94, 111.62, 38.53, 34.22, 33.32, 33.01, 31.91, 29.71, 28.75, 26.50, 23.75, 23.07, 22.71, 14.16, 14.15. MALDI-TOF MS (m/z):  $\text{C}_{45}\text{H}_{57}\text{Br}_2\text{NO}_2\text{S}_2$  ( $\text{M}^+$ ) calc. 932.00, found 931.71.

**P1.** To a mixture of M1 (80 mg, 0.086 mmol), FBDT-Sn (80.7 mg, 0.086 mmol),  $\text{Pd}_2(\text{dba})_3$  (2.4 mg, 0.0026 mmol) and  $\text{P}(\text{o-tol})_3$  (7.8 mg, 0.026 mmol) in a Schlenk flask was added toluene (0.8 mL) under argon. The mixture was heated to reflux for 16 h. Then, 8 mL chlorobenzene was added and the mixture was stirred at 110 °C for 10 min. The solution was added into 100 mL methanol dropwise. The precipitate was collected and further purified via Soxhlet extraction by using  $\text{CH}_2\text{Cl}_2$ ,  $\text{CH}_2\text{Cl}_2$ : $\text{CHCl}_3$  (1:1),  $\text{CHCl}_3$  in sequence. The chloroform fraction was concentrated and added into methanol dropwise. The precipitate was collected and dried under vacuum overnight to give **P1** as a brown solid (89 mg, 75%). The  $M_n$  for P1 is 69.7 kDa, with a PDI of

1.73.  $^1\text{H}$  NMR ( $\text{CDCl}_3$ , 400 MHz,  $\delta/\text{ppm}$ ): 7.95-6.84 (br, aromatic protons), 3.39-2.87 (br, aliphatic protons), 1.54-0.88 (br, aliphatic protons).

#### 4. NMR

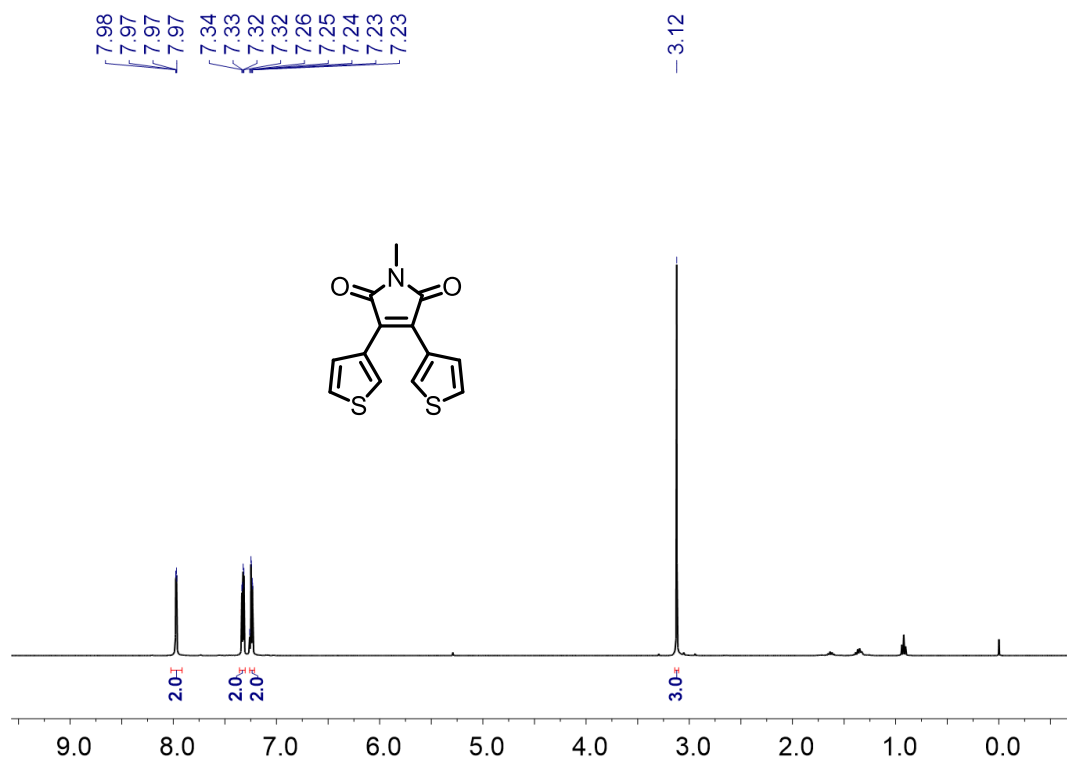


Fig. S2 <sup>1</sup>H NMR spectrum of compound 1.

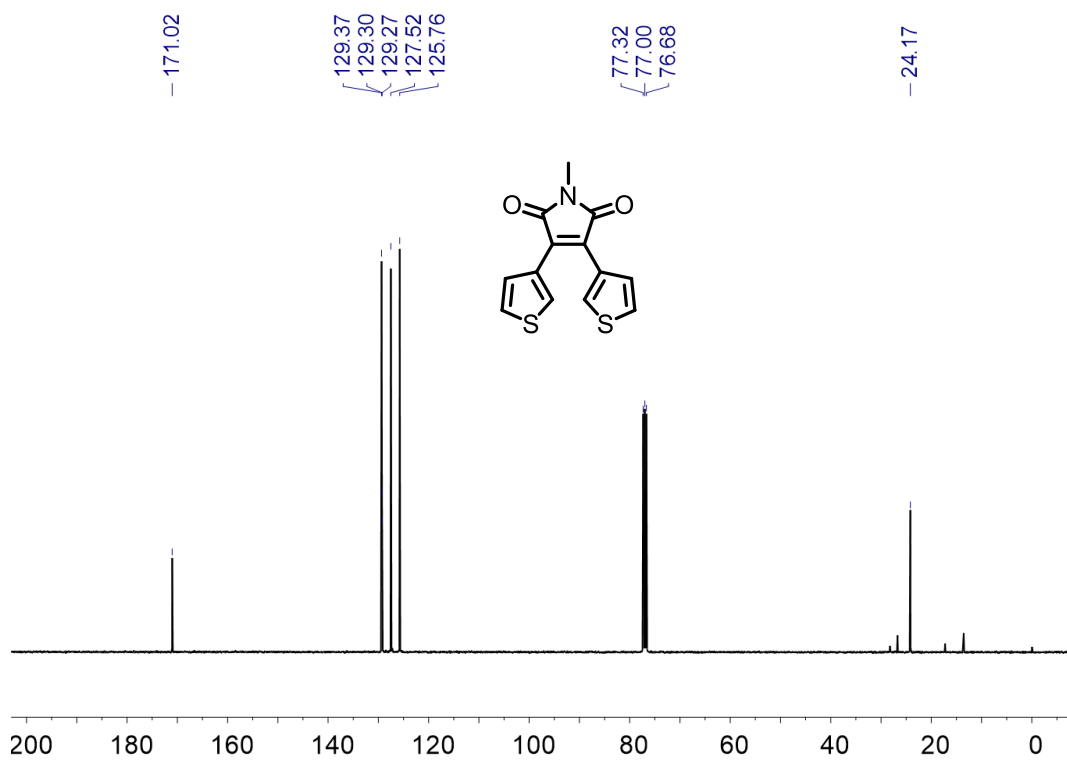
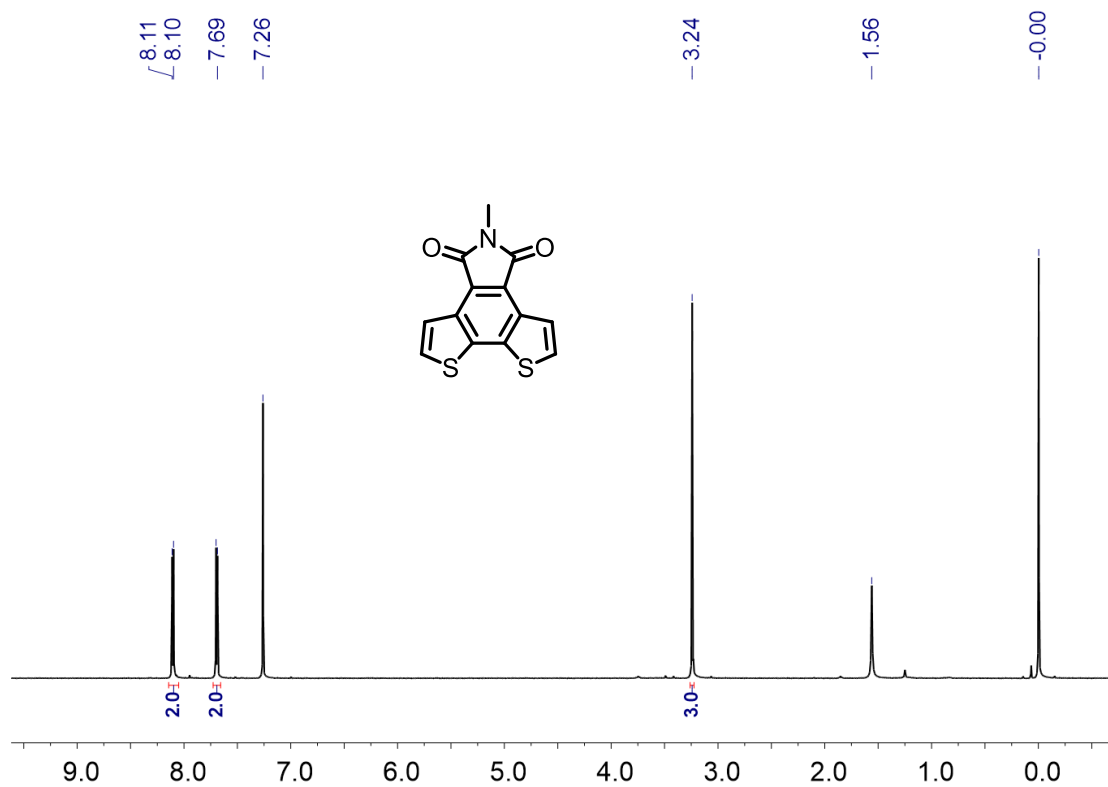
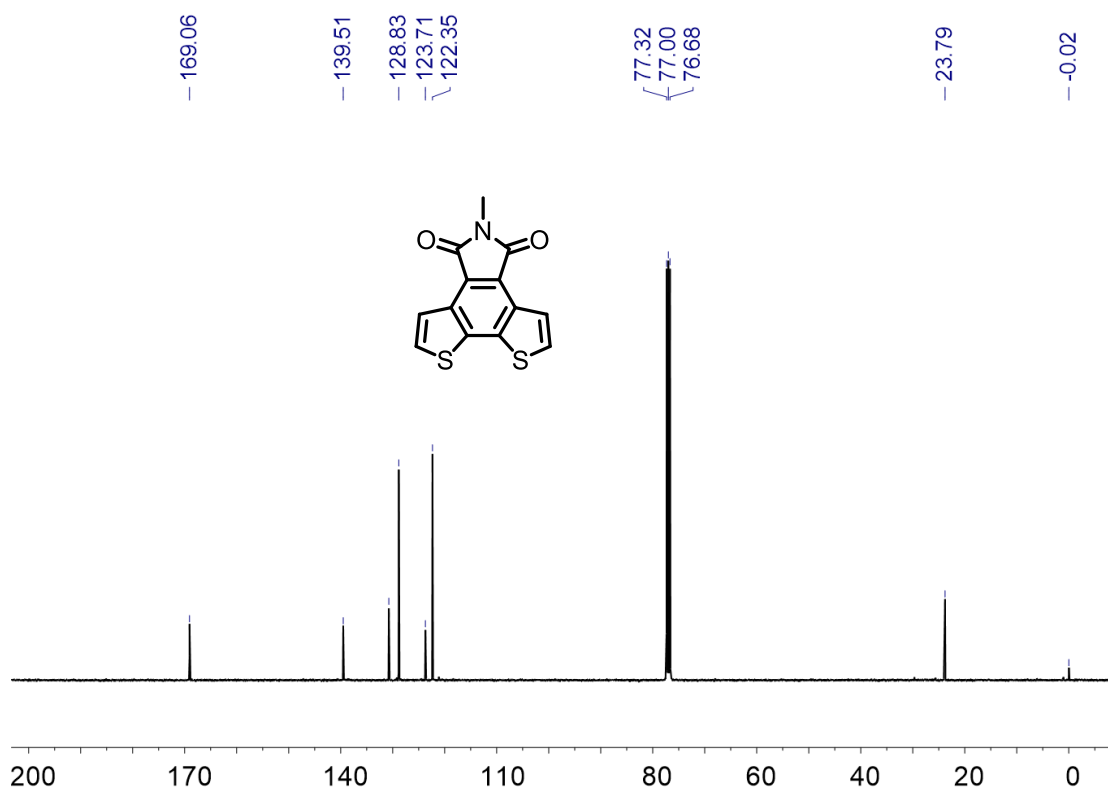


Fig. S3 <sup>13</sup>C NMR spectrum of compound 1.



**Fig. S4**  $^1\text{H}$  NMR spectrum of MDTID.



**Fig. S5**  $^{13}\text{C}$  NMR spectrum of MDTID.

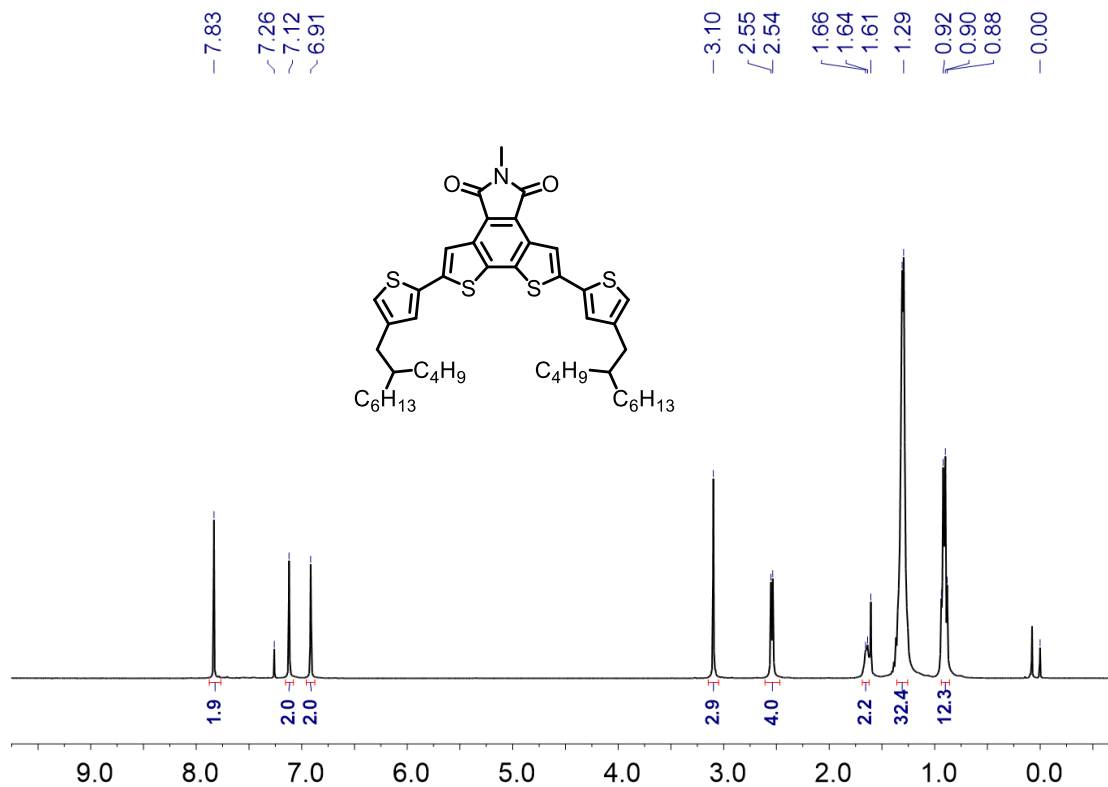


**Fig. S6** <sup>1</sup>H NMR spectrum of **compound 2**.

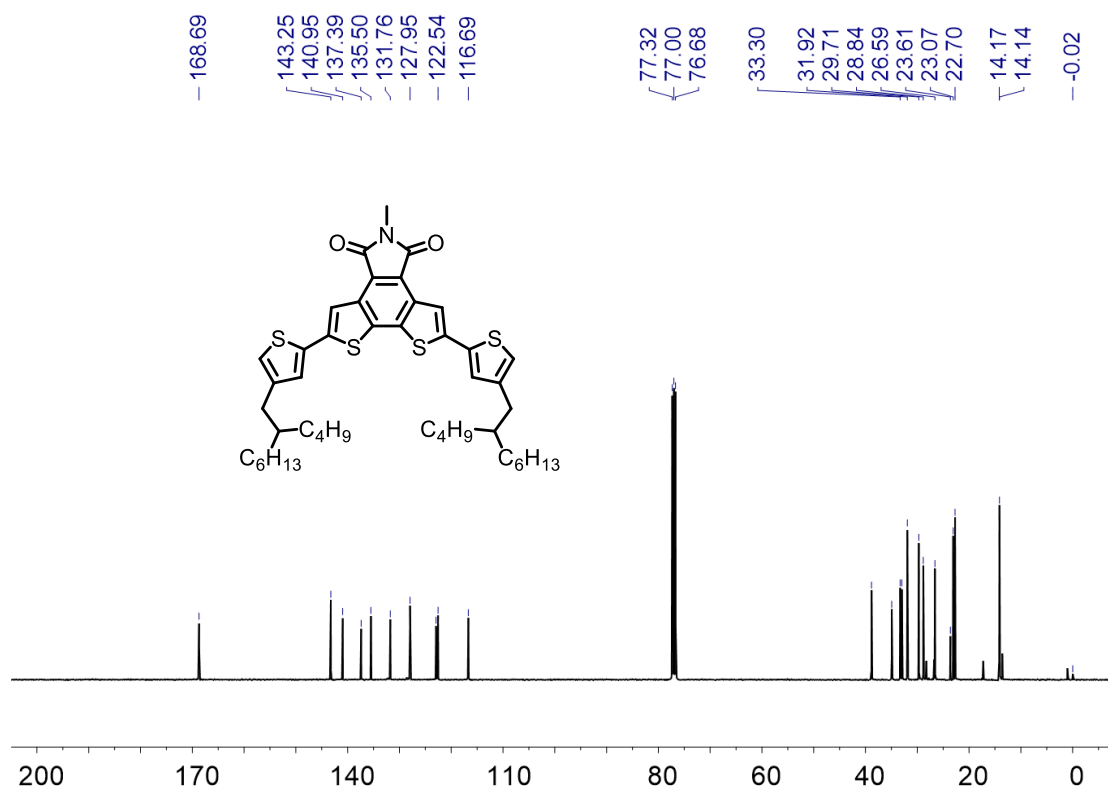


**Fig. S7** <sup>13</sup>C NMR spectrum of **compound 2**.

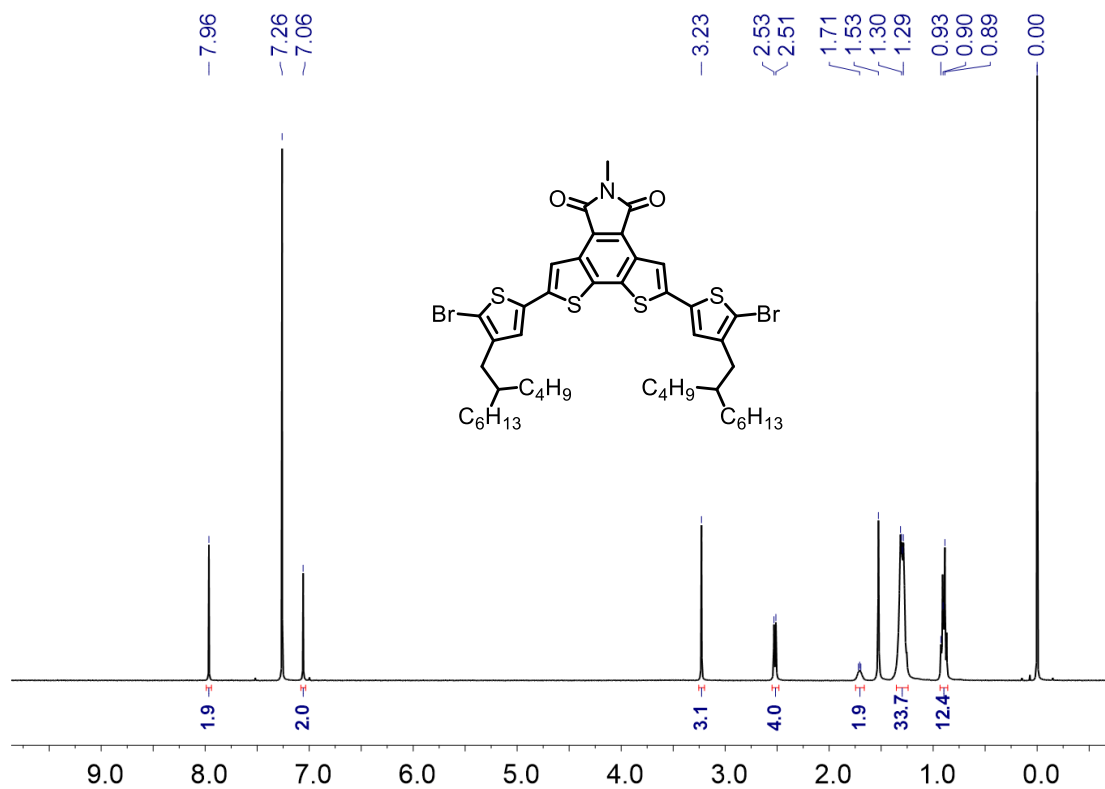


Fig. S8  $^1\text{H}$  NMR spectrum of M1.

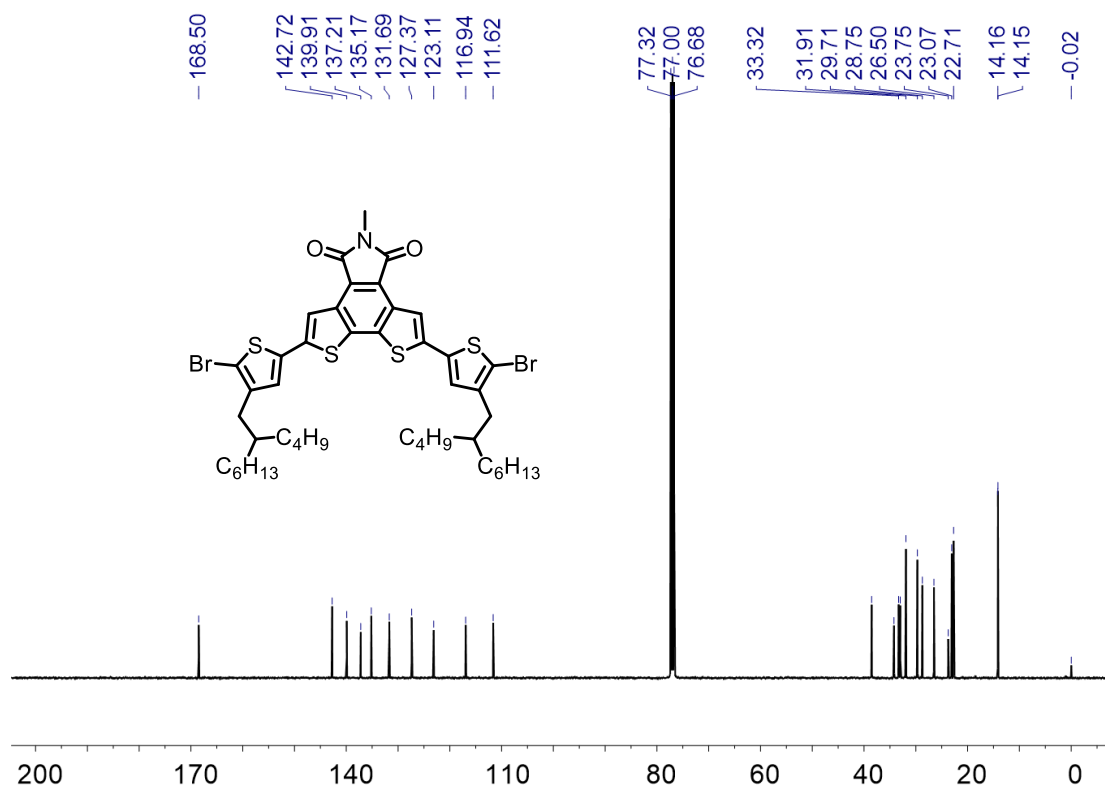
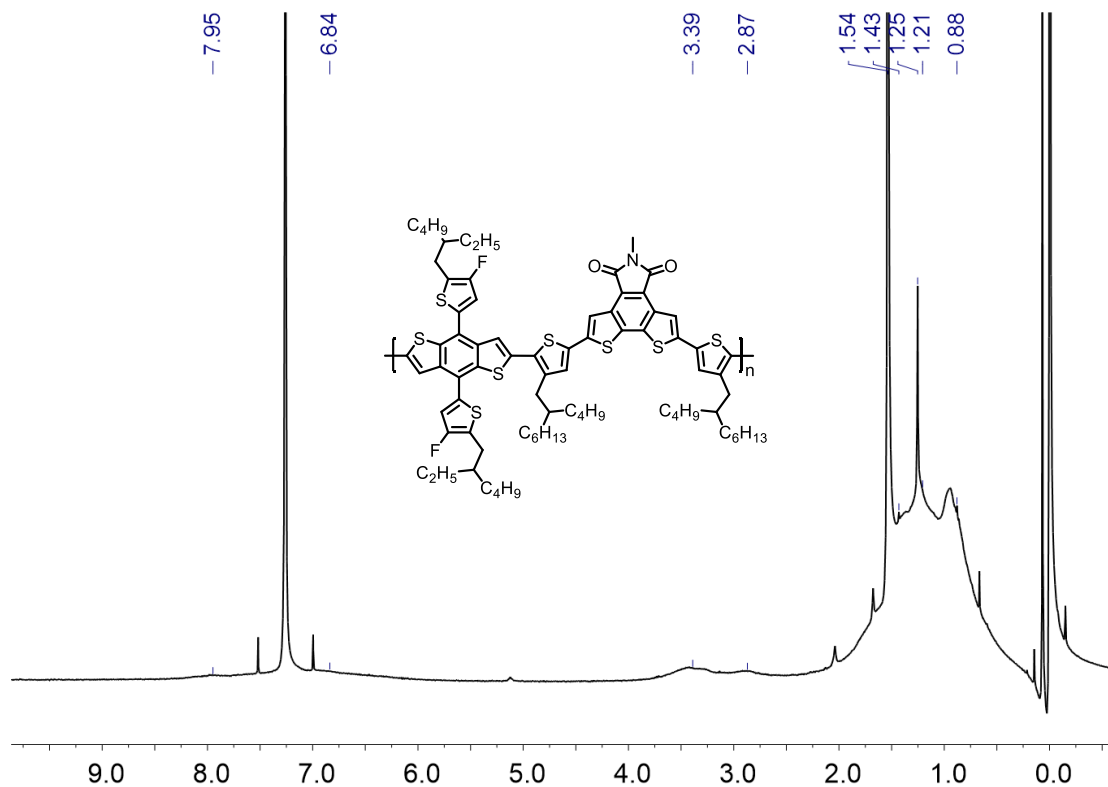
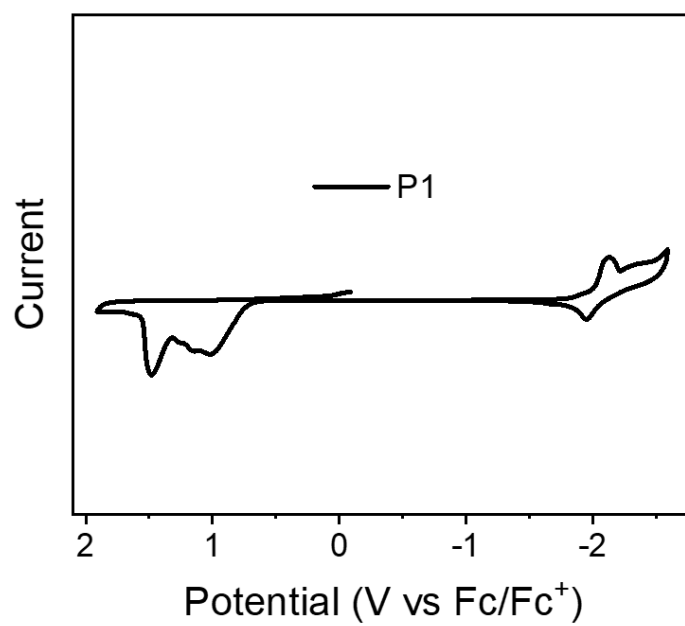


Fig. S9  $^{13}\text{C}$  NMR spectrum of M1.



**Fig. S10**  $^1\text{H}$  NMR spectrum of P1.

## 5. CV



**Fig. S11** Cyclic voltammogram for P1.

## 6. Energy levels

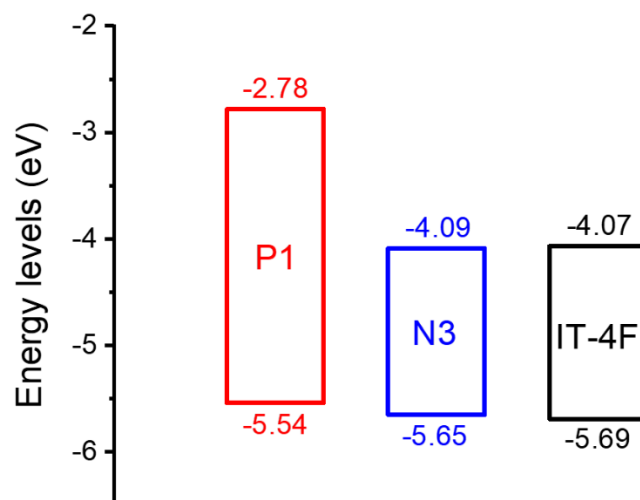


Fig. S12 HOMO and LUMO levels for P1, N3<sup>[1]</sup> and IT-4F<sup>[2]</sup>.

## 7. Device fabrication and measurements

### Conventional solar cells

A 30 nm thick PEDOT:PSS layer was made by spin-coating an aqueous dispersion onto ITO glass (4000 rpm for 30 s). PEDOT:PSS substrates were dried at 150 °C for 10 min. A P1:N3 blend in chloroform (CF) (or a P1:IT-4F blend in chlorobenzene (CB)) was spin-coated onto PEDOT:PSS. PDIN (2 mg/mL) in MeOH:AcOH (1000:3) was spin-coated onto active layer (5000 rpm for 30 s). Ag (~80 nm) was evaporated onto PDIN through a shadow mask (pressure ca.  $10^{-4}$  Pa). The effective area for the devices is 4 mm<sup>2</sup>. The thicknesses of the active layers were measured by using a KLA Tencor D-120 profilometer. *J-V* curves were measured by using a computerized Keithley 2400 SourceMeter and a Xenon-lamp-based solar simulator (Enli Tech, AM 1.5G, 100 mW/cm<sup>2</sup>). The illumination intensity of solar simulator was determined by using a monocrystalline silicon solar cell (Enli SRC2020, 2cm×2cm) calibrated by NIM. The external quantum efficiency (EQE) spectra were measured by using a QE-R3011 measurement system (Enli Tech).

### Hole-only devices

The structure for hole-only devices is ITO/PEDOT:PSS/active layer/MoO<sub>3</sub>/Al. A 30 nm thick PEDOT:PSS layer was made by spin-coating an aqueous dispersion onto ITO glass (4000 rpm for 30 s). PEDOT:PSS substrates were dried at 150 °C for 10 min. A pure P1 in CF (or a P1:N3 blend in CF; or a P1:IT-4F blend in CB) was spin-coated onto PEDOT:PSS. Finally, MoO<sub>3</sub> (~6 nm) and Al (~100 nm) was successively evaporated onto the active layer through a shadow mask (pressure ca.  $10^{-4}$  Pa). *J-V* curves were measured by using a computerized Keithley 2400

SourceMeter in the dark.

### **Electron-only devices**

The structure for electron-only devices is Al/active layer/Ca/Al. Al (~80 nm) was evaporated onto a glass substrate. A P1:N3 blend in CF (or a P1:IT-4F blend in CB) was spin-coated onto Al. Ca (~5 nm) and Al (~100 nm) were successively evaporated onto the active layer through a shadow mask (pressure ca.  $10^{-4}$  Pa).  $J$ - $V$  curves were measured by using a computerized Keithley 2400 SourceMeter in the dark.

## 8. Optimization of device performance

**Table S1** Optimization of D/A ratio for P1:N3 conventional solar cells.<sup>a</sup>

D/A [w/w]	$V_{oc}$ [V]	$J_{sc}$ [mA/cm <sup>2</sup> ]	FF [%]	PCE [%]
1:0.8	0.92	22.26	54.8	11.23 (11.11) <sup>b</sup>
1:1.2	0.90	24.52	65.8	14.52 (14.25)
1:1.6	0.90	24.47	62.7	13.81 (13.68)
1:2	0.90	24.19	63.2	13.77 (13.51)

<sup>a</sup>Blend solution: 14.5 mg/mL in CF; spin-coating: 4000 rpm for 30 s.

<sup>b</sup>Data in parentheses are averages for 8 cells.

**Table S2** Optimization of active layer thickness for P1:N3 conventional solar cells.<sup>a</sup>

Thickness [nm]	$V_{oc}$ [V]	$J_{sc}$ [mA/cm <sup>2</sup> ]	FF [%]	PCE [%]
145	0.90	22.98	56.4	11.66 (11.36) <sup>b</sup>
115	0.91	24.09	61.2	13.42 (13.28)
100	0.90	24.52	65.8	14.52 (14.25)
85	0.91	23.60	64.4	13.83 (13.62)
70	0.91	23.20	64.2	13.55 (13.47)

<sup>a</sup>D/A ratio: 1:1.2 (w/w); blend solution: 14.5 mg/mL in CF.

<sup>b</sup>Data in parentheses are averages for 8 cells.

**Table S3** Optimization of DIO content for P1:N3 conventional solar cells.<sup>a</sup>

DIO [vol%]	$V_{oc}$ [V]	$J_{sc}$ [mA/cm <sup>2</sup> ]	FF [%]	PCE [%]
0	0.90	24.52	65.8	14.52 (14.25) <sup>b</sup>
0.1	0.91	24.86	62.6	14.16 (13.82)
0.3	0.90	24.81	56.6	12.64 (12.50)
0.5	0.90	24.18	54.5	11.86 (11.62)

<sup>a</sup>D/A ratio: 1:1.2 (w/w); blend solution: 14.5 mg/mL in CF; spin-coating: 4000 rpm for 30 s.

<sup>b</sup>Data in parentheses stand are averages for 8 cells.

**Table S4** Optimization of D/A ratio for P1:IT-4F conventional solar cells.<sup>a</sup>

D/A [w/w]	$V_{oc}$ [V]	$J_{sc}$ [mA/cm <sup>2</sup> ]	FF [%]	PCE [%]
1:0.8	0.96	17.60	54.7	9.24 (9.03) <sup>b</sup>
1:1.2	0.97	18.50	56.9	10.21 (10.04)
1:1.6	0.97	16.77	59.9	9.74 (9.48)
1:2	0.96	15.16	59.7	8.67 (8.46)

<sup>a</sup>Blend solution: 15.6 mg/mL in CB; spin-coating: 4000 rpm for 30 s.

<sup>b</sup>Data in parentheses are averages for 8 cells.

**Table S5** Optimization of active layer thickness for P1:IT-4F conventional solar cells.<sup>a</sup>

Thickness [nm]	$V_{oc}$ [V]	$J_{sc}$ [mA/cm <sup>2</sup> ]	FF [%]	PCE [%]
160	0.95	17.29	45.8	7.52 (7.35) <sup>b</sup>
135	0.96	18.38	52.1	9.19 (8.87)
115	0.97	18.50	56.9	10.21 (10.04)
95	0.96	18.14	56.7	9.87 (9.65)
80	0.96	17.29	58.5	9.71 (9.45)

<sup>a</sup>D/A ratio: 1:1.2 (w/w); blend solution: 15.6 mg/mL in CB.

<sup>b</sup>Data in parentheses are averages for 8 cells.

**Table S6** Optimization of DIO content for P1:IT-4F conventional solar cells.<sup>a</sup>

DIO [vol%]	$V_{oc}$ [V]	$J_{sc}$ [mA/cm <sup>2</sup> ]	FF [%]	PCE [%]
0	0.97	18.50	56.9	10.21 (10.04) <sup>b</sup>
0.3	0.95	19.63	66.3	12.36 (12.17)
0.5	0.95	20.31	64.6	12.46 (12.29)
0.7	0.92	13.12	39.2	4.73 (4.52)

<sup>a</sup>D/A ratio: 1:1.2 (w/w); blend solution: 15.6 mg/mL in CB; spin-coating: 4000 rpm for 30 s.

<sup>b</sup>Data in parentheses stand are averages for 8 cells.

## 9. SCLC

Charge carrier mobility was measured by SCLC method. The mobility was determined by fitting the dark current to the model of a single carrier SCLC, which is described by:

$$J = \frac{9}{8} \varepsilon_0 \varepsilon_r \mu \frac{V^2}{d^3}$$

where  $J$  is the current density,  $\mu$  is the zero-field mobility of holes ( $\mu_h$ ) or electrons ( $\mu_e$ ),  $\varepsilon_0$  is the permittivity of the vacuum,  $\varepsilon_r$  is the relative permittivity of the material,  $d$  is the thickness of the blend film, and  $V$  is the effective voltage ( $V = V_{\text{appl}} - V_{\text{bi}}$ , where  $V_{\text{appl}}$  is the applied voltage, and  $V_{\text{bi}}$  is the built-in potential determined by electrode work function difference). Here,  $V_{\text{bi}} = 0.1$  V for hole-only devices,  $V_{\text{bi}} = 0$  V for electron-only devices.<sup>[3]</sup> The mobility was calculated from the slope of  $J^{1/2}$ - $V$  plot.

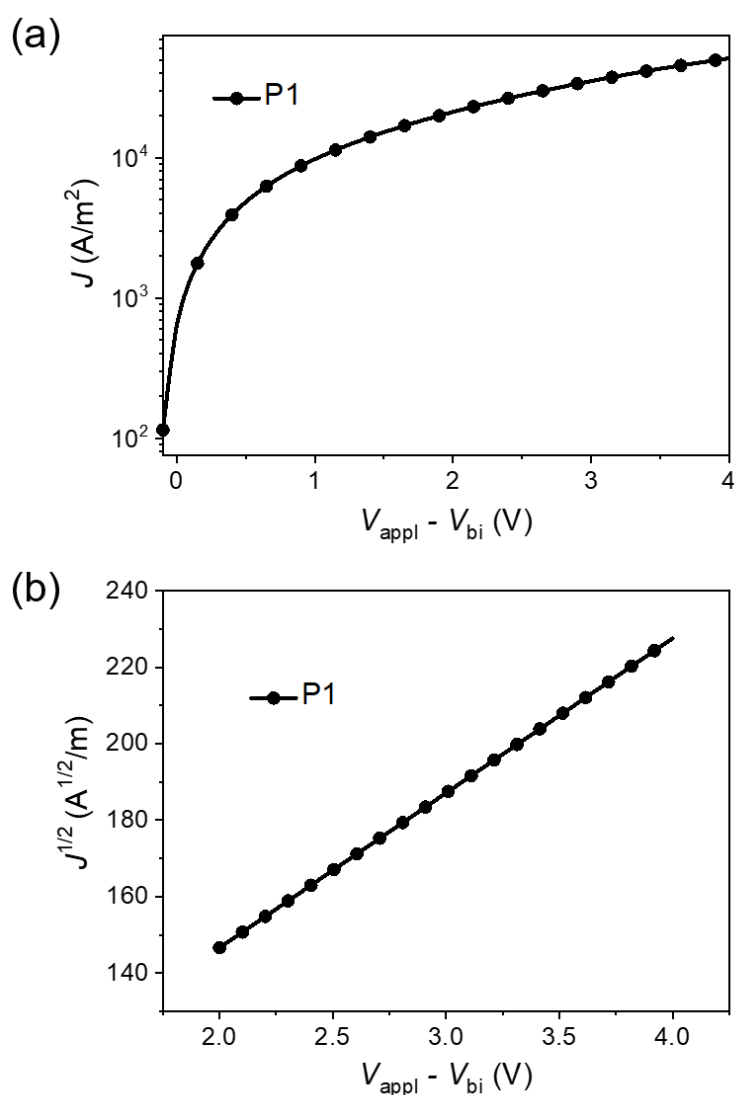


**Fig. S13**  $J$ - $V$  curve (a) and corresponding  $J^{1/2}$ - $V$  plot (b) for the hole-only devices (in dark). The thickness for P1 pure film is 109 nm.

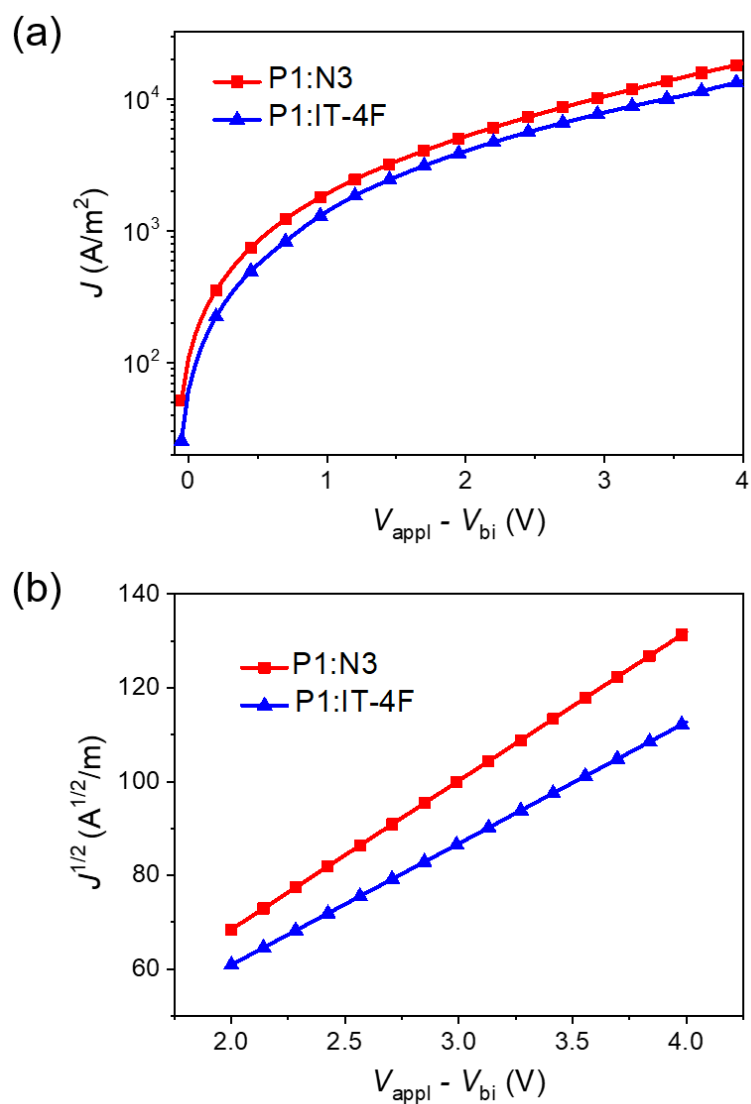


**Fig. S14**  $J$ - $V$  curves (a) and corresponding  $J^{1/2}$ - $V$  plots (b) for the hole-only devices (in dark). The thicknesses for P1:N3 and P1:IT-4F films are 105 nm and 103 nm, respectively.

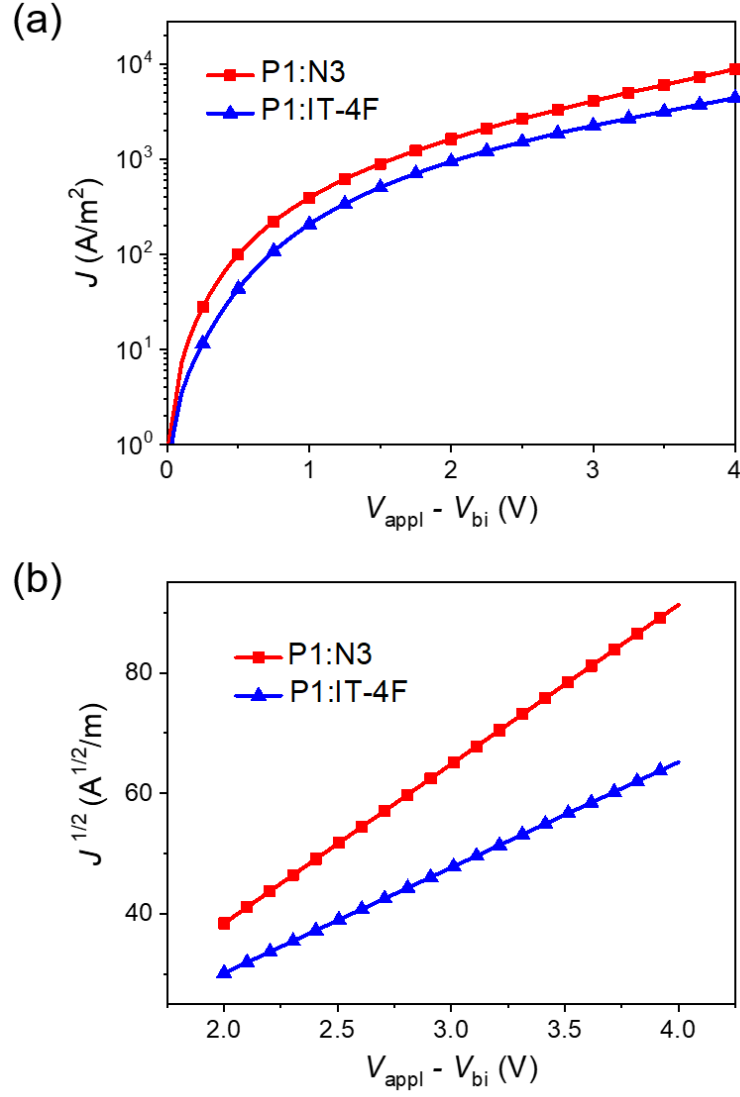


**Fig. S15**  $J$ - $V$  curves (a) and corresponding  $J^{1/2}$ - $V$  plots (b) for the electron-only devices (in dark). The thicknesses for P1:N3 and P1:IT-4F films are 104 and 105 nm, respectively.

**Table S7** Hole and electron mobilities.

Films	$\mu_h$ [cm <sup>2</sup> /Vs]	$\mu_e$ [cm <sup>2</sup> /Vs]	$\mu_h/\mu_e$
P1	$7.10 \times 10^{-4}$	-	-
P1:N3 (1:1.2)	$3.90 \times 10^{-4}$	$2.63 \times 10^{-4}$	1.48
P1:IT-4F (1:1.2)	$2.45 \times 10^{-4}$	$1.19 \times 10^{-4}$	2.06

## 10. Bimolecular recombination

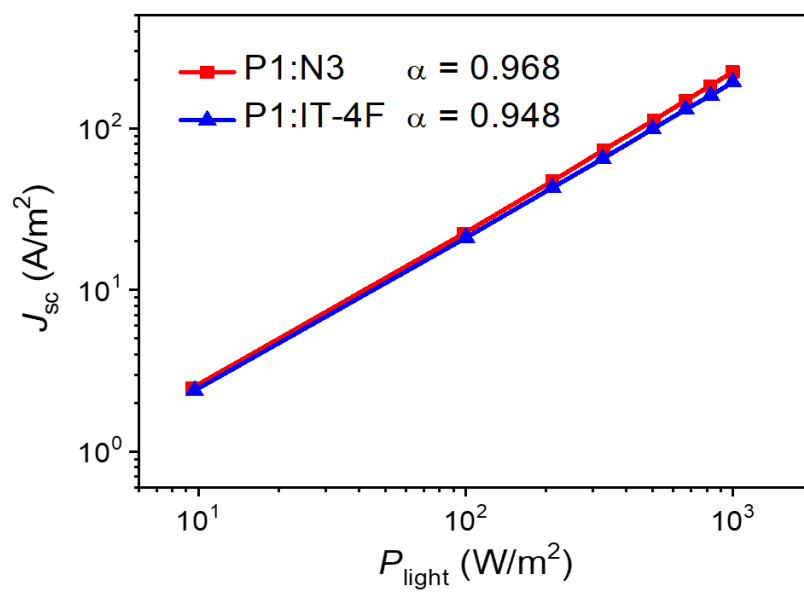


**Fig. S16**  $J_{sc}$ - $P_{light}$  plots.

## 11. AFM

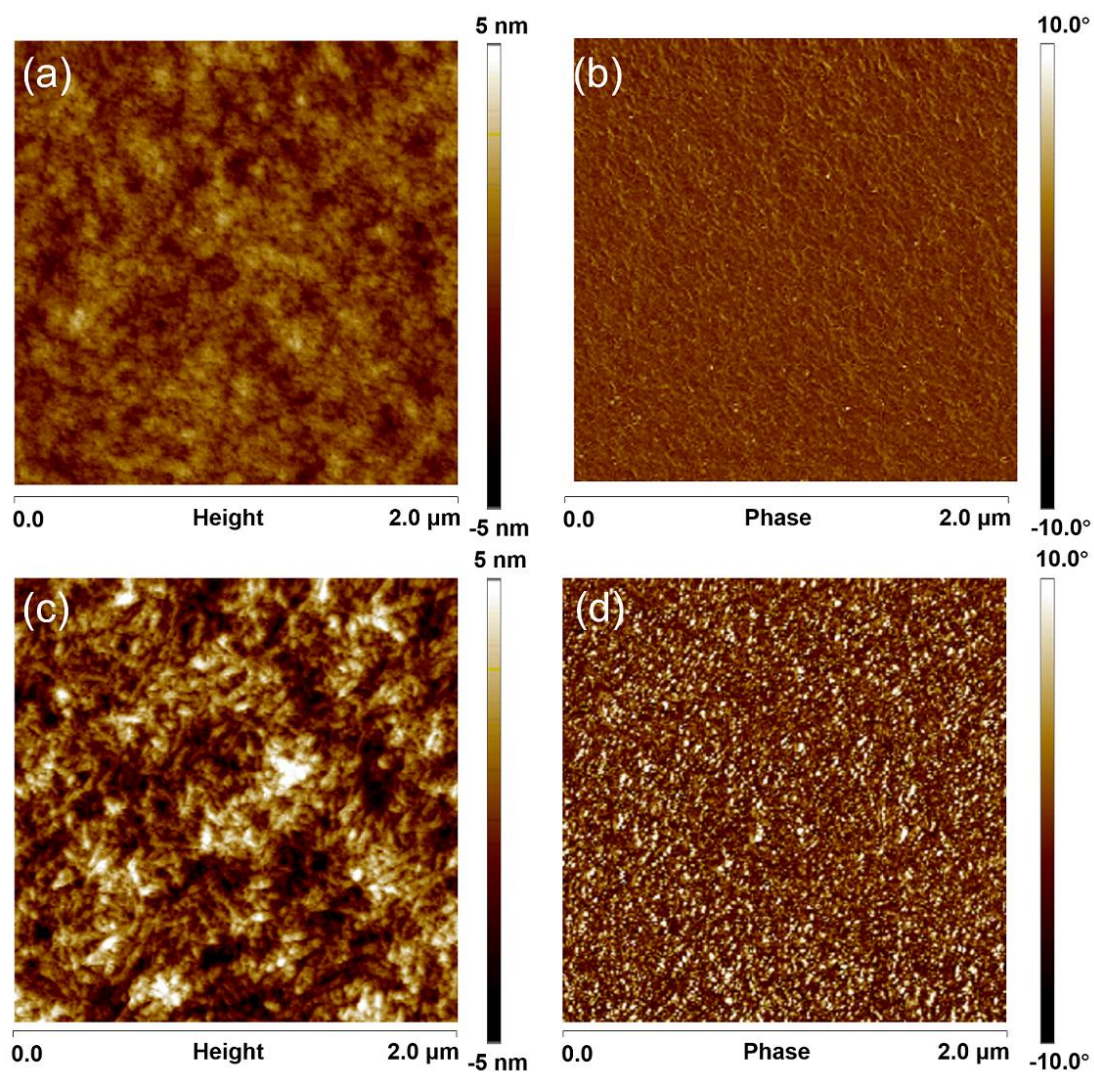


**Fig. S17** AFM height (left) and phase (right) images for the blend films. (a) and (b), P1:N3 and film ( $R_{\text{rms}} = 0.80$  nm); (c) and (d), P1:IT-4F film ( $R_{\text{rms}} = 1.76$  nm).  $R_{\text{rms}}$ : root-mean-square roughness.

## References

- [1] S. Li, C.-Z. Li, M. Shi and H. Chen, New Phase for Organic Solar Cell Research: Emergence of Y-Series Electron Acceptors and Their Perspectives, *ACS Energy Lett.*, 2020, **5**, 1554-1567.
- [2] Y. Yi, Q. Liang, L. Li, J. Liu and Y. Han, Constructing interpenetrating network of polymer/non-fullerene blend system by small molecule preferential crystallization, *Chin. J. Appl. Chem.*, 2019, **36**, 424-430.
- [3] C. Duan, W. Cai, B. B. Y. Hsu, C. Zhong, K. Zhang, C. Liu, Z. Hu, F. Huang, G. C. Bazan, A. J. Heeger and Y. Cao, Toward green solvent processable photovoltaic materials for polymer solar cells: the role of highly polar pendant groups in charge carrier transport and photovoltaic behavior, *Energy Environ. Sci.*, 2013, **6**, 3022-3034.